# Dynamics of proton migration and dissociation in core-excited ethyne probed by multiple ion momentum imaging

J. Laksman , D. Céolin, M. Gisselbrecht, S. E. Canton, and S. L. Sorensen

Citation: The Journal of Chemical Physics **131**, 244305 (2009); doi: 10.1063/1.3270159
View online: http://dx.doi.org/10.1063/1.3270159
View Table of Contents: http://aip.scitation.org/toc/jcp/131/24
Published by the American Institute of Physics

# Dynamics of proton migration and dissociation in core-excited ethyne probed by multiple ion momentum imaging

J. Laksman,[1,a)] D. Céolin,[1] M. Gisselbrecht,[1] S. E. Canton,[2] and S. L. Sorensen[1]
[1]*Department of Synchrotron Radiation Research, University of Lund, S-221 00 Lund, Sweden*
[2]*Department of Chemical Physics, University of Lund, S-221 00 Lund, Sweden*

(Received 18 September 2009; accepted 10 November 2009; published online 29 December 2009)

The study focuses on the rapid geometry change in ethyne excited near the carbon 1*s* edge. Core excitation and ionization lead to population of dicationic states in ethyne. We study three competing dissociation pathways associated with deprotonation in the linear ethyne molecule, and two cases of rapid proton migration. We investigate the alignment of the molecule in the excited state and find startling differences in these three cases. We present evidence for a strong anisotropy in the production of $H_2^+/C_2^+$ fragments through a rapid deformation of the molecule to a dibridged conformation with the transition dipole moment parallel to the polarization of the exciting radiation. © *2009 American Institute of Physics*. [doi:10.1063/1.3270159]

Ethyne has become a model system for studying photoinduced nuclear dynamics due mainly to its linear geometry, the importance of proton migration in chemistry, and to the relative simplicity of the ethyne molecule.[1] A large number of experimental and theoretical studies have focused on characterizing the electronic states involved in isomerization to vinylidene in the valence region, especially in the cation and dicationic species (see Ref. 2). The existence of the vinylidene isomer was confirmed by UV photoelectron spectroscopy of the ethyne anion by Ervin,[3] and the barrier for proton migration was calculated to be a few kcal/mol for the ground state. Theory predicts several energetically favorable paths leading to a vinylidene geometry,[4,5] and a novel transition state was recently suggested by the study of Palaudoux.[6] The experimental ion-ion coincidence study by Thissen[7] identified the thresholds for several dication fragmentation channels in the valence region, and found that rearrangement to vinylidene is possible after photoexcitation around 34 eV. Ethyne core-excited states were studied extensively using the ARPIS method where fragment ion are measured to extract the symmetry of core-excited states,[8–10] and Gadea *et al.*[11] discussed the implications of fast proton migration in the core-excited state. Osipov found a proton migration time of about 60 fs for the core-ionized state[12] in accord with the time scale found in pump-probe studies.[13] The ground state of the ethyne molecule is linear with $D_{\infty h}$ symmetry, but the C $1s^{-1}\pi^{*1}$ core-excited state has a bent equilibrium geometry.[14] The absorption spectrum near the C 1*s* edge also shows evidence of excited bending modes[15] and Adachi recently used photoelectron-ion-ion coincidences to show the role of core-hole localization in bond breaking.[16] The recent study by Kimberg *et al.*[17] made the connection between the core-excited state and the alignment of bonds in the final dicationic state, and they described the role of the core-hole lifetime and the transition dipole moment in detail.

In the present investigation, we concentrate our study on ethyne dication produced after C 1*s* electron excitation to the $\pi_g^*$ valence orbital. The core-excited state decays rapidly via Auger transitions, which populate electronic states in the dication, and dissociation to two or more fragments can result. By analyzing the momenta of all fragments produced in dissociation we can filter out events connected with isomerization and deformation from the linear geometry. We discuss two-body dissociation of the ethyne dication in the context of fast proton migration, focusing on the $C_2^+/H_2^+$ and $CH_2^+/C^+$ fragmentation channels. We find that these channels show distinctly different alignments in fragmentation. The molecular alignment in the dissociative dicationic state is measured and a connection to channels in the core-excited state is discussed.

A multiple-ion coincidence momentum imaging spectrometer was developed in order to study fragmentation of molecules and clusters. It is based on a design by Prümper *et al.*, that has been presented in detail in Ref. 18, and has been characterized using the SIMION package.[19] The time-of-flight spectrometer has a two stage acceleration and one drift tube and is equipped with an electrostatic lens that focuses ions onto an 80 mm diameter two-dimensional position sensitive detector (ROENTDEK DLD80). Voltages are chosen to optimize collection efficiency. The 10 ns dead time imposes no constraints since the peaks presented in this study do not overlap.

The measurements were performed at the soft x-ray beamline I411 at MAX-laboratory in Lund, Sweden.[20] The degree of linear polarization is measured to be at least 99.5%. The spectrometer axis is mounted at 90° with respect to the horizontal polarization axis. The sample gas pressure in the spectrometer chamber was $5\times10^{-6}$ mbar. A total ion yield spectrum of ethyne was recorded, and a photoenergy calibration was made at the C $1s\rightarrow\pi_g^\star$ resonance after comparison to the spectrum in Ref. 14. Few multiple ion coincidences were detected in the off-resonance spectrum at 270 eV, indicating a negligible contribution from second-order light. From the total ion yield we find an off/on resonance intensity ratio that is $\leq 1/15$, showing that the direct valence shell photoemission can be neglected in our study.

a)Electronic mail: joakim.laksman@sljus.lu.se.

 

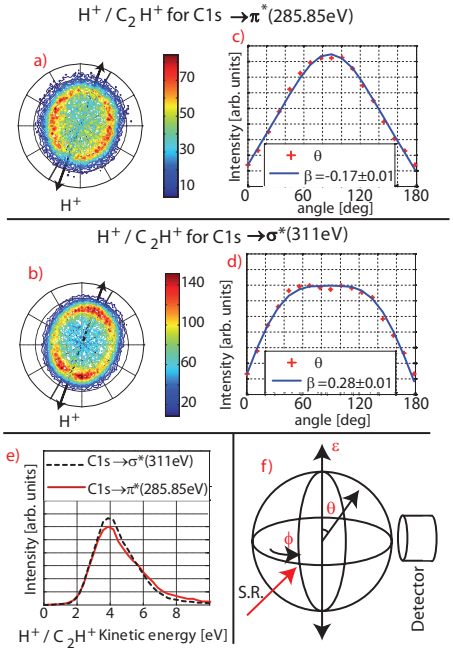


FIG. 1. Experimental data on the $H^+/C_2H^+$ two-body dissociation channel. The polar plots show the location of the $H^+$ ions for (a) the C $1s \rightarrow \pi^*$ resonance at 285.85 eV and (b) at 311 eV, which corresponds to the C $1s \rightarrow \sigma^*$ resonance. In the lower half of (b) an intensity anomaly can be seen intersecting $\vec{\epsilon}$, that is due to the injection needle. The direction of the polarization vector is shown in the plots. The $\beta$-parameter reduces the spherical angle distribution to one numerical value. (c) and (d) show histograms of the zenith angular distribution, $\theta$, with which $\beta$ has been estimated. The normalized total kinetic energy released to the fragment pair for these two cases is shown in (e). (f) shows that $\theta$ is defined with respect to the polarization vector $\vec{\epsilon}$. $\phi$ is the azimuth angle. The synchrotron radiation (SR) is perpendicular to $\vec{\epsilon}$ and the detector axis.

Our study includes measurements of two-body dissociation from all of the core-excited states, below resonance, and for ionization in the vicinity of the $\sigma^*$ shape resonance at 311 eV. In Fig. 1 double coincidence data from the deprotonation channel, $H^+/C_2H^+$, are presented. This ion pair is a reference for other measurements, considering that it comes from a simple two-body breakup where no proton migration has occurred. The angular distribution of the $H^+$ fragment from each event is plotted on a polar plot in Figs. 1(a) and 1(b) and the distributions for the $\pi^*$ and $\sigma^*$ resonances are shown. In the lower half of polar plots an intensity anomaly can be seen intersecting $\vec{\epsilon}$, that is due to field distortion from the grounded injection needle. The radius of the distribution reflects the kinetic energy, and the angular distribution with respect to the polarization axis reflects the molecular alignment. After transformation into three-dimensional momentum space, estimation of the molecular anisotropy parameter, $\beta$, that ranges from $-1$ for a purely perpendicular transition to 2 for a purely parallel transition was made with a least square fit of the zenith angular distribution [see Fig. 1(f)], $I(\theta)$. The conventional analytical expression is

$$\frac{d\sigma}{d\Omega} = \frac{\sigma}{4\pi}[1 + \beta P_2(\cos\,\theta)], \tag{1}$$

where $d\sigma$ is the differential cross section, $d\Omega$ is the solid angle unit, $\sigma$ is the total cross section integrated over space, and $P_2$ is the second-order Legendre polynomial, $P_2(x) = (3x^2-1)/2$. The observed intensity of $I(\theta)$ then follows from an integration over the azimuth angle $\phi$,[21]

$$I(\theta) = \frac{\sigma}{4\pi}\int [1 + \beta P_2(\cos\,\theta)]d\Omega, \tag{2}$$

where $d\Omega = \sin\,\theta d\theta d\phi$, so

$$I(\theta) = \frac{\sigma}{4\pi}\int_0^{2\pi} d\phi \int_{\theta}^{\theta+\Delta\theta} d\theta \sin\,\theta[1 + \beta P_2(\cos\,\theta)] \tag{3}$$

with the solution

$$I(\theta) = \frac{\sigma}{2}\sin\,\theta[1 + \beta P_2(\cos\,\theta)]. \tag{4}$$

For double coincidences, $\theta$ is the mean value. Error estimation of $\beta$ was made with residual analysis, so that the residuals do not deviate by more than 10% from their minimum value. In the analysis of the angular distribution of fragments the position-dependent efficiency of the detector must be characterized. Measurement of the ion distribution after ionization by unpolarized light gives the value $\beta=0$ of the anisotropy parameter, indicating a uniform detector efficiency. The $\beta$ for $H^+/C_2H^+$ is $-0.17$ for $\pi^*$ and 0.28 for $\sigma^*$, see Figs. 1(c) and 1(d). These values are in qualitative agreement with the expected alignment, but nonetheless far from purely anisotropic. Kimberg showed that stretching modes do not produce a deviation from the initial orientation,[17] so we conclude that bending modes have a significant impact.

We measure a relatively strong signal from the $C^+$ and $CH_2^+$ pair at all photon energies, in accord with the results reported in earlier studies.[4,5,7] The data shown in Fig. 2 in-

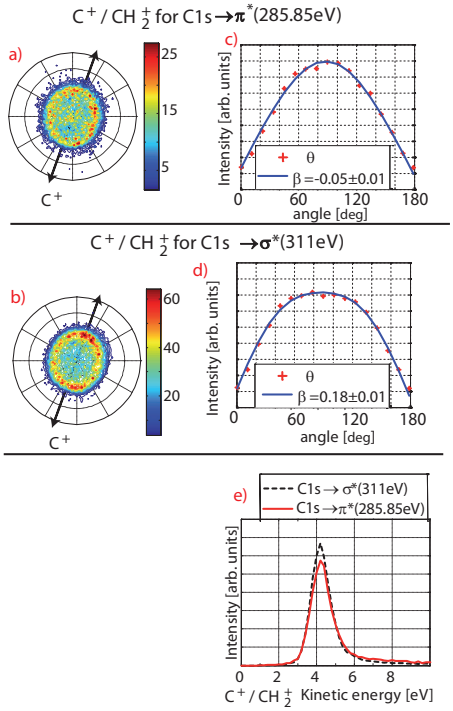


FIG. 2. Experimental data on the $C^+/CH_2^+$ two-body dissociation channel. The polar plots show the location of the $C^+$ ions which arrive in coincidence with $CH_2^+$ ions for (a) the C $1s \rightarrow \pi^*$ resonance at 285.85 eV and (b) at 311 eV. (c) and (d) present the $\beta$ parameters. The total kinetic energy released to the fragments is shown in (e).

dicate a very weak dependence on the core-excited state for that channel. $\beta$ is found to be nearly isotropic for $C^+/CH_2^+$ at the C $1s \rightarrow \pi_g^*$ resonance and for the C $1s \rightarrow \sigma^*$ resonance we find $\beta$=0.18. The kinetic energy released (KER) shows a relatively narrow distribution in both cases, with a peak at around 4.3 eV [Fig. 2(e)]. For both energies, the KER is essentially identical.

The threshold for this reaction is at 34.0 eV, and valence photoionization produces a KER of 4.5 at 40 eV.[7] The calculated energy of the transition state for vinylidene is 34.5 eV. Duflot[4] found two possible routes leading to this fragment pair. The ground state of the ethyne dication ($^3\Sigma_g^-$) is correlated with a planar transition state with a low activation barrier, resulting in a lengthening of the CH bond. The first excited state of the ethyne dication, $^1\Delta_g$, on the other hand, correlates to a nonplanar transition state which lengthens the C≡C bond. This transition state has a higher barrier, and Zyubina *et al.*[5] found that this route is favored in the case of low internal energy, while the previous route is essentially independent of the internal energy. In a recent Auger electron-ion-ion coincidence study by Flammini[2] the Auger electrons coinciding with the $^1\Delta_g$ state were associated with the $C^+$ and $CH_2^+$ fragment pair. Clearly this state is populated after core-electron ionization, but a significant population is reached even from the core-excited state.

Osipov *et al.*[12] showed that both the $^1\Delta_g$ and the $^1\Sigma_g^+$ states in the dication lead to the $C^+/CH_2^+$ ion pair, but the path via the $^1\Sigma_g^+$ state is predicted to dominate the decay. Calculations of the potential surfaces predict a KER of 4.25 eV. The total measured energy released in the reaction [Fig. 2(e)] has a peak at 4.3 eV, which corresponds very well to the prediction of Osipov. This energy distribution is independent of the core-excited state, and as outlined by Kimberg *et al.*[17] is due primarily to the difference between the energy of the dication of the vinylidene and the fragments. The proton migration leading to vinylidene formation and the measurement of its subsequent dissociation indicates that the memory of the C≡C alignment given by the core excitation is lost. We can compare this case to the study by Kimberg,[17] where proton emission at the C $1s \rightarrow \pi^*$ resonance maximum had an experimental anisotropy of about −0.38. The discrepancy from their theoretical value of $\beta \approx -0.6$ was explained with two possibilities: either it was due to undetected low-energetic cations or due to the potential energy surface of the dissociative state being different from that of the excited state. In our measurement all kinetic energies are gathered, and our maximum is at $\beta$=−0.32, which is close enough to the value of Kimberg to exclude the explanation of low-energetic fragments.

Another two-body dissociation channel, which results from hydrogen migration, is the $H_2^+$ and $C_2^+$ pair. This pair is found nearly exclusively at the C $1s^{-1}\pi_g^{*1}$ state and shows a strong asymmetry along the direction of the polarization of the exciting radiation [see Fig. 3(a)]. For the C $1s \rightarrow 3s\sigma_g/3\sigma_u^*$ transition, the lack of observation of this pair is surprising, considering their coupling with the C $1s^{-1}\pi_g^{*1}$ excited state through the bending vibrations.[9,10,16] This asymmetry is very different than the measurements of the $C^+/CH_2^+$ pair. The measured coincidence data at the C $1s^{-1}\pi^{*1}$ and C $1s^{-1}\sigma^{*1}$ are presented in Fig. 3. The $\beta$ values for these two measurements differ dramatically, with a value close to 1 for the $\pi^*$ resonance and for $\sigma^*$ we find −0.58. Note that this channel is very weak for the 311 eV case, but the asymmetry is clearly visible. The data for the kinetic energy released are less reliable for the 311 eV ionization.

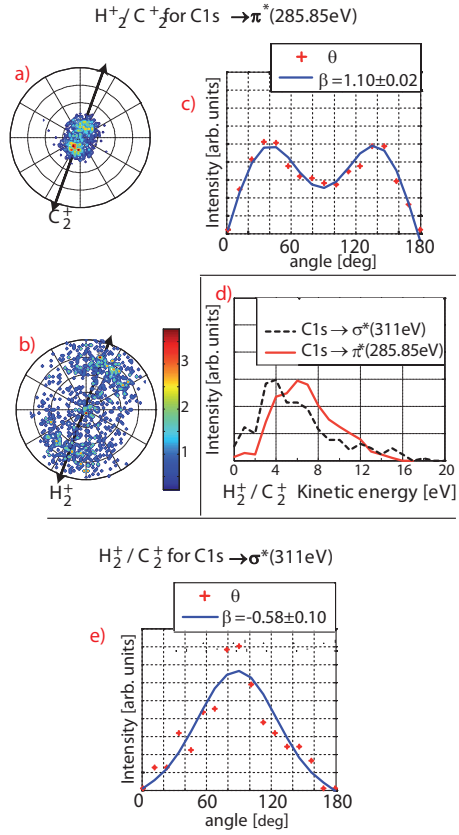


FIG. 3. Experimental data on the $H_2^+/C_2^+$ two-body dissociation channel. (a) and (b) show the location of the $H_2^+$ and $C_2^+$ ions for the C $1s \rightarrow \pi^*$ resonance at 285.85 eV. A histogram of their average angular distribution is plotted in (c) from which $\beta$ has been extracted. $\beta$ for C $1s \rightarrow \sigma^*$ is found in (e). The total kinetic energy released to the fragments for these two cases is shown in (d).

In an earlier study the strong deformation of the linear ethyne molecule was connected to the $\nu_5$ *cis* bending mode,[22] and an analysis of the triple coincidences from $C_2H_2^{3+}$ was made to support this. In the present study we focus on the dication, which has been thoroughly described in several theoretical studies.[4–6,12,17] Several studies suggest that the vinylidene structure may have a global energy minimum for the C $1s^{-1}\pi_g^{*1}$ state,[15] and Gadea[11] predicts that the core-excited state may rapidly rearrange to the energetically favorable *cis* bent configuration within the core-hole lifetime. This may lead to population of final dicationic states, which differs substantially from the decay of ethyne in a linear geometry. Palaudoux and Hochlaf[6] identified a dibridged configuration with a *cis* configuration in the dication which correlates to $C_2^+(a^2\Pi_u^+)+H_2^+(X^2\Sigma_g^+)$. This reaction occurs on the lowest singlet potential surface after elongation of both the C≡C bond and the C—H bonds. Their model indicates that this channel competes with the dissociation producing $C_2/2H^+$ fragments, which is also accessible on the same potential energy surface. The proton pair channel was detected

in Thissens study, but the $C_2^+$ and $H_2^+$ channel was not. Although we can detect this pair at 311 eV our measurement indicates that it is strongly populated mainly via the C $1s \rightarrow \pi_g^*$ resonance. Piancastelli *et al.*[23] found in their partial ion yield study of ethyne that the peak in the $H_2^+$ spectrum was slightly narrower than the peak in the $H^+$ spectrum, and the origin of this difference was suggested to be due to the need to populate higher vibrational modes in order to produce a recombination fragment. The beta parameter estimated from the $H_2^+/C_2^+$ channel is explained by the nuclear dynamics in the C $1s^{-1}\pi_g^{*1}$ state. The selection of a specific channel gives us important information not only on the final state dissociation but tells us that the nuclear motion in the core excited state and the photon absorption process cannot be regarded as separate for this particular case. Indeed, at the time of the excitation, photoabsorption triggers the nuclear motion. Among these, the *cis* bending mode can be excited and the corresponding transition dipole moment is in-plane and perpendicular to the C—C bond. By selecting the $H_2^+/C_2^+$ channel, we only monitor molecules undergoing a *cis* motion (as described in Fig. 1 in Ref. 22), with a transition dipole moment aligned with the polarization axis. The subsequent dissociation retains the memory of this alignment, which is reflected in the intensity distribution of the $H_2^+/C_2^+$ fragments, parallel to the polarization vector, $\vec{\epsilon}$. The twofold degeneracy of the C $1s^{-1}\pi^{*1}$ excited state is removed by the vibronic coupling with bending vibrational modes via the Renner–Teller effect. Kempgens *et al.*[15] showed that vibronic coupling in ethyne is responsible for the strong excitation of both the *cis* and *trans* bending modes. The excited state is split into two stable geometries, and Kimberg *et al.*[17] calculate that these states lead to dissociation with very different proton recoil anisotropy parameters. Since the $\beta$ parameter reaches its minimum at the C $1s \rightarrow \pi_g^*$ resonance at 285.85 eV, the $H_2^+/C_2^+$ pair intensity is also expected to have a minimum there. Unfortunately, due to the low intensity of this channel we are not able to extract reliable branching ratios for different excitation energies within the C $1s \rightarrow \pi_g^*$ resonance. According to the study of Kimberg[17] only bending modes change the angular anisotropy. The strong deformation evidenced by the $H_2^+/C_2^+$ channel arises when the *cis* bending mode is excited. The decay must then proceed via Auger transitions to the doubly ionized states, specifically to the lowest triplet level $^3\Sigma_g^-$ and the $^1\Delta_g$ states, which are correlated both to the dibridged conformation, and to the $H_2^+/C_2^+$ dissociation.[6] According to our previous discussion, the $H_2^+/C_2^+$ channel indicates that the dipole moment is mainly perpendicular to the C≡C bond axis. For the $CH_2^+/C^+$ channel the angular anisotropy is zero, indicating that proton transfer instead smears out any alignment in the core-excited state. The fact that $\beta$ for the dibridged channel in Fig. 3(c) is not identical to 2, suggests the presence of a contribution with isotropic distribution. The presence of $H_2^+/C_2^+$ from vinylidene poses a possible explanation, but false coincidences that make up ~9% of the intensity for this weak pathway do also contribute.

In conclusion, we find that the angular anisotropy of ions emitted after core-valence excitation in ethyne provides evidence for deformation of the linear molecule in the excited state. Regarding the $H_2^+/C_2^+$ channel, we conclude that the deformation, that is due to a *cis* bending mode, is fast, and takes place before the electronic decay of the core excited state. Calculations might be interesting to confirm the role of the dipole moment alignment in the interpretation of the $\beta$.

We acknowledge help from MAX laboratory staff and the financial support from Knut and Alice Wallenberg Foundation, the Göran Gustafsson Foundation, and the Swedish Research Council (VR).

[1] S. P. So, R. W. Wetmore, and H. F. Schaefer, J. Chem. Phys. **73**, 5706 (1980).
[2] E. Flammini, E. Farinelli, F. Maracci, and L. Avaldi, Phys. Rev. A **77**, 044701 (2008).
[3] K. Ervin, J. Ho, and W. C. Lineberger, J. Chem. Phys. **91**, 5974 (1989).
[4] D. Duflot, J.-M. Robbe, and J.-P. Flament, J. Chem. Phys. **102**, 355 (1995).
[5] T. S. Zyubina, Y. A. Dyakov, S. H. Lin, A. D. Bandrauk, and A. M. Mebel, J. Chem. Phys. **123**, 134320 (2005).
[6] J. Palaudoux and M. Hochlaf, J. Chem. Phys. **126**, 044302 (2007).
[7] R. Thissen, J. Delwiche, J. M. Robbe, D. Duflot, J. P. Flament, and J. H. D. Eland, J. Chem. Phys. **99**, 6590 (1993).
[8] J. Adachi, N. Kosugi, E. Shigemasa, and A. Yagishita, Chem. Phys. Lett. **309**, 427 (1999).
[9] S. Masuda, T. Gejo, M. Hiyama, and N. Kosugi, J. Electron. Spectrosc. Relat. Phenom. **144–147**, 215 (2005).
[10] N. Kosugi, J. Electron. Spectrosc. Relat. Phenom. **144–147**, 1203 (2005).
[11] F. X. Gadea, S. Mathieu, and L. S. Cederbaum, J. Mol. Struct. THEOCHEM **401**, 15 (1997).
[12] T. Osipov, T. N. Rescigno, T. Weber, S. Miyabe, T. Jahnke, A. S. Alnaser, M. P. Hertlein, O. Jagutzki, L. Ph. H. Schmidt, M. Schöffler, L. Foucar, S. Schössler, T. Havermeier, M. Odenweller, S. Voss, B. Feinberg, A. L. Landers, M. H. Prior, R. Dörner, C. L. Cocke, and A. Belkacem, J. Phys. B **41**, 091001 (2008).
[13] A. Hishikawa, A. Matsuda, E. J. Takahashi, and M. Fushitani, J. Chem. Phys. **122**, 151104 (2005).
[14] Y. Ma, C. T. Chen, G. Meigs, K. Randall, and F. Sette, Phys. Rev. A **44**, 1848 (1991).
[15] B. Kempgens, B. S. Itchkawitz, J. Feldhaus, A. M. Bradshaw, H. Köppel, M. Döscher, F. X. Gadea, and L. S. Cederbaum, Chem. Phys. Lett. **277**, 436 (1997).
[16] J. Adachi, K. Hosaka, T. Teramoto, M. Yamazaki, N. Watanabe, M. Takahashi, and A. Yagishita, J. Phys. B **40**, F285 (2007).
[17] V. Kimberg, N. Kosugi, and F. Gel'mukhanov, J. Chem. Phys. **130**, 114302 (2009).
[18] G. Prümper, H. Fukuzawa, T. Lischke, and K. Ueda, Rev. Sci. Instrum. **78**, 083104 (2007).
[19] D. A. Dahl, SIMION 3D version 7.0 User's Manual, Idaho National Engineering and Environmental Laboratory, 2000.
[20] M. Bässler, A. Ausmees, M. Jurvansuu, R. Feifel, J. O. Forsell, P. de Tarso Fonseca, A. Kivimäki, S. Sundin, S. L. Sorensen, R. Nyholm, O. Björneholm, S. Aksela, and S. Svensson, Nucl. Instrum. Methods Phys. Res. A. **469**, 382 (2001).
[21] A. I. Chichinin, T. S. Einfeld, K. H. Gericke, and C. Maul, in *Imaging in Molecular Dynamics*, edited by B. Whitaker (Cambridge University Press, Cambridge, 2003), pp. 153–155.
[22] N. Saito, M. Nagoshi, M. Machida, I. Koyano, A. De Fanis, and K. Ueda, Chem. Phys. Lett. **393**, 295 (2004).
[23] M. N. Piancastelli, W. C. Stolte, G. Öhrwall, S.-W. Yu, D. Bull, K. Lantz, A. S. Schlachter, and D. W. Lindle, J. Chem. Phys. **117**, 8264 (2002).